
Genomic Analysis of Murine Pulmonary Tissue Following Carbonyl Chloride Inhalation

**Alfred M. Sciuto, Christopher S. Phillips, Linda D. Orzolek,
Alison I. Hege, Theodore S. Moran, and James F. Dillman III**

Neurotoxicology Branch and Applied Pharmacology Branch,
Pharmacology Division, U.S. Army Medical Research Institute of
Chemical Defense, Aberdeen Proving Ground, Maryland 21010-5400

**Chemical
Research in
Toxicology[®]**

Reprinted from
Volume 18, Number 11, Pages 1654–1660

Genomic Analysis of Murine Pulmonary Tissue Following Carbonyl Chloride Inhalation

Alfred M. Sciuto,^{*,†} Christopher S. Phillips,[‡] Linda D. Orzolek,[‡] Alison I. Hege,[‡] Theodore S. Moran,[‡] and James F. Dillman III[‡]

Neurotoxicology Branch and Applied Pharmacology Branch, Pharmacology Division,
U.S. Army Medical Research Institute of Chemical Defense,
Aberdeen Proving Ground, Maryland 21010-5400

Received May 10, 2005

Carbonyl chloride (phosgene) is a toxic industrial compound widely used in industry for the production of synthetic products, such as polyfoam rubber, plastics, and dyes. Exposure to phosgene results in a latent (1–24 h), potentially life-threatening pulmonary edema and irreversible acute lung injury. A genomic approach was utilized to investigate the molecular mechanism of phosgene-induced lung injury. CD-1 male mice were exposed whole body to either air or a concentration \times time amount of 32 mg/m³ (8 ppm) phosgene for 20 min (640 mg \times min/m³). Lung tissue was collected from air- or phosgene-exposed mice at 0.5, 1, 4, 8, 12, 24, 48, and 72 h postexposure. RNA was extracted from the lung and used as starting material for the probing of oligonucleotide microarrays to determine changes in gene expression following phosgene exposure. The data were analyzed using principal component analysis to determine the greatest sources of data variability. A three-way analysis of variance based on exposure, time, and sample was performed to identify the genes most significantly changed as a result of phosgene exposure. These genes were rank ordered by *p* values and categorized based on molecular function and biological process. Some of the most significant changes in gene expression reflect changes in glutathione synthesis and redox regulation of the cell, including upregulation of glutathione S-transferase α -2, glutathione peroxidase 2, and glutamate-cysteine ligase, catalytic subunit (also known as γ -glutamyl cysteine synthetase). This is in agreement with previous observations describing changes in redox enzyme activity after phosgene exposure. We are also investigating other pathways that are responsive to phosgene exposure to identify mechanisms of toxicity and potential therapeutic targets.

Introduction

Physiological and molecular mechanisms of toxic industrial gas inhalation remain to be determined. For many toxic industrial chemicals (TICs),^{1,2} treatment after exposure continues to be fundamentally anecdotal due to the uncertainty of the type of gas and the duration and concentration of exposure. Assessment of lung pulmonary injury is critical for the development of rational medical countermeasures. In this study, we determined the temporal molecular response of murine pulmonary tissue after inhalation of the toxic industrial gas carbonyl chloride (phosgene, CAS no. 75-44-5).

Phosgene, an irritant gas, is used as a chemical intermediate for the production of synthetic materials. It has been estimated that over one million tons of phosgene are used in the United States each year (1).

Toxic phosgene concentrations can also be produced through the thermal decomposition of chlorinated hydrocarbons (2). The potential for accidental exposure is not limited to the United States. In some areas of Europe, because of heavy industrialization and proximity to populated areas, phosgene has been identified as an environmental hazard (3). Taken all together, there exists the potential for accidental environmental and/or occupational exposure to this TIC. Exposure to phosgene gas has long been known to cause latent noncardiogenic pulmonary edema in both man and experimental models. Mechanisms of toxicity are gradually being resolved (4). Elucidation of the mechanisms of phosgene toxicity is important not only because of the exposure hazards but also because it is considered to be a potential terrorist threat since it is simple and inexpensive to produce.

We have previously established that phosgene inhalation causes a multitude of pathological, physiological, biochemical, and toxicological disturbances in both lung tissue and bronchoalveolar lavage fluid (BALF) across a range of animal models (5–12). These data consistently indicate that the primary effect of phosgene exposure is on the GSH redox cycle that is critical in the detoxification of free radical-mediated tissue and cellular injury (5, 13). The most prominent physiological effects occur within the first 8 h after exposure, resulting in the common observation of enhanced BALF protein levels,

* To whom correspondence should be addressed. Tel: 410-436-5115. Fax: 410-436-2750. E-mail: alfred.mario.sciuto@us.army.mil.

[†] Neurotoxicology Branch.

[‡] Applied Pharmacology Branch.

¹ Abbreviations: BALF, bronchoalveolar lavage fluid; GPx, glutathione peroxidase; GR, glutathione reductase; GS, glutathione synthetase; SOD3, superoxide dismutase 3; GCL, glutamate cysteine ligase; GST, glutathione-S-transferase; Q-PCR, quantitative real-time polymerase chain reaction; PCA, principal component analysis; TIC, toxic industrial chemical.

² The data discussed in this publication have been deposited in NCBI's Gene Expression Omnibus (GEO, <http://www.ncbi.nlm.nih.gov/geo/>) and are accessible through GEO Series accession no. GSE2565.

REPORT DOCUMENTATION PAGE

Form Approved
OMB No. 0704-0188

Public reporting burden for this collection of information is estimated to average 1 hour per response, including the time for reviewing instructions, searching existing data sources, gathering and maintaining the data needed, and completing and reviewing this collection of information. Send comments regarding this burden estimate or any other aspect of this collection of information, including suggestions for reducing this burden to Department of Defense, Washington Headquarters Services, Directorate for Information Operations and Reports (0704-0188), 1215 Jefferson Davis Highway, Suite 1204, Arlington, VA 22202-4302. Respondents should be aware that notwithstanding any other provision of law, no person shall be subject to any penalty for failing to comply with a collection of information if it does not display a currently valid OMB control number. **PLEASE DO NOT RETURN YOUR FORM TO THE ABOVE ADDRESS.**

1. REPORT DATE (DD-MM-YYYY) 2005		2. REPORT TYPE Open literature article		3. DATES COVERED (From - To)	
4. TITLE AND SUBTITLE Genomic Analysis of Murine Pulmonary Tissue Following Carbonyl Chloride Inhalation				5a. CONTRACT NUMBER	
				5b. GRANT NUMBER	
				5c. PROGRAM ELEMENT NUMBER	
6. AUTHOR(S) Sciuto, AM, Phillips, CS, Orzolek, LD, Hege, AI, Moran, TS, Dillman JF, III				5d. PROJECT NUMBER	
				5e. TASK NUMBER	
				5f. WORK UNIT NUMBER	
7. PERFORMING ORGANIZATION NAME(S) AND ADDRESS(ES) US Army Medical Research Institute of Chemical Defense ATTN: MCMR-CDT-T 3100 Ricketts Point Road Aberdeen Proving Ground, MD 21010-5400				8. PERFORMING ORGANIZATION REPORT NUMBER USAMRICD-P05- 04 ⁰¹⁴	
9. SPONSORING / MONITORING AGENCY NAME(S) AND ADDRESS(ES) US Army Medical Research Institute of Chemical Defense ATTN: MCMR-CDA-T 3100 Ricketts Point Road Aberdeen Proving Ground, MD 21010-5400				10. SPONSOR/MONITOR'S ACRONYM(S)	
				11. SPONSOR/MONITOR'S REPORT NUMBER(S)	
12. DISTRIBUTION / AVAILABILITY STATEMENT Approved for public release; distribution unlimited					
13. SUPPLEMENTARY NOTES Published in Chemical Research in Toxicology, 18(11), 1654-1660, 2005					
14. ABSTRACT See reprint					
15. SUBJECT TERMS phosgene, inhalation, microarray analysis, gene expression profiling					
16. SECURITY CLASSIFICATION OF:			17. LIMITATION OF ABSTRACT UNLIMITED	18. NUMBER OF PAGES 7	19a. NAME OF RESPONSIBLE PERSON Alfred M. Sciuto
a. REPORT UNCLASSIFIED	b. ABSTRACT UNCLASSIFIED	c. THIS PAGE UNCLASSIFIED			19b. TELEPHONE NUMBER (include area code) 410-436-5115

increased pulmonary edema, and ultimately decreased survival rates (9, 14). While we have identified several prominent biochemical pathways involved in phosgene toxicity, we have not established the molecular mechanisms that activate these pathways. One component of this may involve regulation of gene expression.

The present study utilized oligonucleotide microarrays to assay global changes in pulmonary gene expression following phosgene inhalation in mice. We identified statistically significant phosgene-induced changes that reflect a number of biological processes perturbed by exposure to this TIC. We determined the temporal effects of phosgene exposure on lung tissue antioxidant enzyme concentrations at the gene expression level, compared these results with those from air-exposed mice treated in a similar manner, and assessed the role of the GSH redox cycle in this oxidative lung injury model. In addition, the present microarray data have been directly linked to the biochemical data from a prior study (21) and show that there is excellent agreement between gene expression analytical techniques and actual biochemical response in an identical exposure model. Clarification of these exposure responses will be useful for development of rational therapeutic strategies and identification of early molecular markers of a TIC-induced acute lung injury.

Experimental Procedures

Phosgene Exposure Model. Forty male Crl:CD-1 (ICR)BR mice (29 ± 1 g, Charles River Laboratories, Wilmington, MA) were exposed whole body to a concentration \times time of 32–42 mg/m^3 (8–11 ppm) phosgene for 20 min (640–840 $\text{mg min}/\text{m}^3$). Exposure of mice to this concentration of phosgene for 20 min results in a $\text{LC}_{50-60\%}$ at 12 h and a $\text{LC}_{60-70\%}$ at 24 h. At the concentration delivered, we routinely observed 50–60% mortality at 12 h and 60–70% mortality at 24 h. Exposure to phosgene was followed by a 5 min room air washout. The total chamber time for air-exposed or phosgene-exposed animals was 25 min. All elements of exposure were performed in an approved laboratory fume hood. Ten percent phosgene/90% N_2 (Matheson Gas Products, Baltimore, MD) was metered through a Tylan mass flow controller (Tylan Corp., Torrance, CA) at a rate dependent on the desired concentration. This was mixed with room air and then passed through an infrared spectrometer (Miran 1A, Foxboro Co., Sharon, MA). The Miran 1A was equipped with a real-time analogue output. The exposure occurred in a Plexiglas cylinder (25 cm in height \times 28 cm in diameter) with a total volume of 15.8 L at a flow rate of 20 L/min. Out-flowing gas from the chamber was passed through a second Miran 1A unit to determine the concentration of phosgene exiting the chamber. Effluent from the hood was passed through an M18 filter and then through standard activated charcoal fume hood filters. A similar group of 40 male mice was exposed whole body to room air for 25 min. Assessment of early molecular markers of air and phosgene exposures was performed in lung tissue harvested at 0.5, 1, 4, 8, 12, 24, 48, and 72 h after exposure. Three mice per time point were sacrificed using 100% CO_2 . Three mice not exposed to either air or phosgene were labeled as “naïve”. These were selected as unexposed baseline biological samples for the air and phosgene-exposed mice. All mice were housed in an accredited AAALAC International animal holding facility with a 12 h day and 12 h night light cycle. Mice were fed and watered ad libitum.

Gene Expression Profiling. All experiments were performed using Affymetrix Mouse 430A oligonucleotide arrays, as described at http://www.affymetrix.com/support/technical/datasheets/mogarrays_datasheet.pdf (Affymetrix, Santa Clara, CA). Frozen mouse lungs were homogenized in Tri Reagent (Sigma-Aldrich Chemical Co., St. Louis, MO), and the total RNA

was extracted according to the manufacturer's protocol (<http://www.sigmaaldrich.com/sigma/bulletin/t9424bul.pdf>). RNA was further purified using RNeasy columns (Qiagen, Valencia, CA). The quality and amount of RNA were monitored throughout processing with an Agilent Bioanalyzer (Agilent, Palo Alto, CA) and a NanoDrop ND-1000 UV–vis spectrophotometer (NanoDrop Technologies, Rockland, DE). Purified RNA was used to prepare biotinylated target RNA, with minor modifications from the manufacturer's recommendations (http://www.affymetrix.com/support/technical/manual/expression_manual.affx). Briefly, 10 μg of total RNA was used to generate first strand cDNA by using a T7-linked oligo(dT) primer. After second strand synthesis, *in vitro* transcription was performed with biotinylated nucleotides (Enzo Diagnostics, Farmingdale, NY). The target cRNA generated from each sample was processed as per manufacturer's recommendation using an Affymetrix GeneChip Instrument System (http://www.affymetrix.com/support/technical/manual/expression_manual.affx). Briefly, spiked controls were added to 15 μg of fragmented cRNA before overnight hybridization using 10 μg of cRNA. Arrays were then washed and stained with streptavidin–phycoerythrin before being scanned on an Agilent GeneArray Scanner. After scanning, array images were assessed by eye to confirm scanner alignment and the absence of significant bubbles or scratches on the chip surface. The 3'/5' ratios for GAPDH were between 0.73 and 2.02, and the ratios for β -actin were between 1.02 and 1.6. BioB spike controls were found to be present on 82 out of 104 chips that were scanned (78.8%), with BioC, BioD, and CreX also present in increasing intensity. When scaled to a target intensity of 150 (using Affymetrix Microarray Suite 5.0 array analysis software), scaling factors for all arrays were between 0.644 and 1.748.

Microarray Data Analysis. To develop a robust data set for subsequent statistical analysis, a sample size of $n = 3$ mice was used for each time and dose indicated ($n = 3$ biological replicates), and probes generated from each sample were used to probe duplicate chips ($n = 2$ chip replicates). Scanned output files from each array were inspected for quality control as described and then processed using Affymetrix Microarray Suite (v 5.0), Affymetrix MicroDB (v3.0), and Affymetrix Data Mining Tool (v 3.0) as described (<http://www.affymetrix.com/index.affx>). The raw data were imported as a comma separated values (.csv) file into Partek Pro 6.0 (Partek, St. Charles, MO). To obtain a data set with a normal distribution for statistical analysis, the raw data were normalized by the addition of a constant ($c = 1$) followed by log transformation (\log_2). The log-transformed data were analyzed by principal component analysis (PCA) to determine the significant sources of variability in the data. This information was used to determine grouping variables for analysis of variance (ANOVA). A three-way mixed model ANOVA was carried out using exposure, time, and sample as grouping variables; sample was coded as a random effect for the ANOVA. A Bonferroni and Dunn–Sidak multiple test correction was performed. A set of genes with significantly altered expression levels based on p values from the ANOVA was visualized using a heat map and used to determine gene pathways and molecular networks significantly affected by phosgene exposure. Onto-Express was used to screen for significant pathways modulated by phosgene exposure (15).

Quantitative Real Time Polymerase Chain Reaction (Q-PCR). All Q-PCR was performed with Taq-Man PCR reagents and analyzed using the ABI 7500 Sequence Detection System (Applied Biosystems, Foster City, CA). All primers and probes used for Q-PCR analysis were designed using ABI Prism Primer Express v. 2.0 (Applied Biosystems) and are listed in Supporting Information Table 1. Primers and probes for each gene were optimized individually for maximum amplification efficiency. A validation experiment was performed to demonstrate that each target gene and endogenous control in a multiplex reaction maintained equal efficiencies. Total RNA was purified as described above and DNase I treated on a purification column according to the manufacturer's protocol (Qiagen). The reverse transcription reaction was carried out using 1 μg of total RNA

(final concentration, 50 ng/ μ L) using SuperScript II reverse transcriptase (Invitrogen, Carlsbad, CA). After completion of cDNA synthesis, all reactions were diluted to a final RNA input concentration of 5 ng/ μ L. For each gene analyzed, the experimental samples being tested (three biological replicates for each treatment group) were run in triplicate (three technical replicates) along with the corresponding no template control and no amplification control. The primer and probe pair concentrations used for each gene are as follows: β -actin (endogenous control), 300 nM forward primer, 300 nM reverse primer, 100 nM VIC probe; SOD3, 300 nM forward primer, 300 nM reverse primer, 250 nM Fam probe; glutathione reductase (GR), 300 nM forward primer, 800 nM reverse primer, 250 nM Fam probe; glutathione synthetase (GS), 800 nM forward primer, 300 nM reverse primer, 200 nM Fam probe; and glutathione peroxidase (GPx), 300 nM forward primer, 300 nM reverse primer, 150 nM Fam probe. Amplification reactions were carried out using the instrument default cycle conditions. β -Actin was used as the internal reference gene to calculate the ΔC_t for each sample assayed. The $\Delta\Delta C_t$ was then calculated based on the average ΔC_t of the naive control samples. The fold change in gene expression was determined as $2^{-\Delta\Delta C_t}$ (16). Dixon's outlier test (extreme value test) was applied to all fold change values for each gene investigated. Samples 112 (1 h air), 135 (24 h air), and 12 (1 h phosgene) were identified as outliers in all genes assayed (level of significance 0.1 for sample 135 for GR, level of significance 0.05 for remaining assays).

Results

PCA. Gene expression data from phosgene-exposed mouse lungs were analyzed by PCA (Supporting Information Figure 1). PCA reduces the complexity of high-dimensional data and simplifies the task of identifying patterns and sources of variability in a large data set. The samples (three biological replicates each hybridized to two separate arrays) are represented by the points in the three-dimensional plot. The distance between any pair of points is related to the similarity between the two observations in high-dimensional space. Samples that are near each other in the plot are similar in a large number of variables (i.e., expression level of individual genes). Conversely, samples that are far apart in the plot are different in a large number of variables. In this data set, the major sources of data variability are linked to exposure (air or phosgene) and time of exposure. No significant data variability was attributed to sample processing, chip lot, or other technical parameters. There is a clear separation of the air-exposed samples as compared with the phosgene-exposed samples regardless of time (Supporting Information Figure 1). When the air-exposed samples and the phosgene-exposed samples are each analyzed separately by PCA, a clear partitioning based on time of exposure is evident in the phosgene-exposed samples (Supporting Information Figure 2). In contrast, there is no clear partitioning of samples based on time in the air-exposed control group. The 48 and 72 h samples are partitioned away from naive controls and away from the other time points, suggesting that even at later time points there is still a significant difference in the gene expression profiles of animals recovering from phosgene exposure out to 72 h.

Validation of Selected Microarray Results by Q-PCR. The reliability of our microarray data was confirmed using Q-PCR analysis of selected oxidant enzyme genes that have been studied previously in phosgene exposure. As shown in Supporting Information Figure 3, the relative expression levels of GPx 2, GR1,

GS, and SOD3 based on Q-PCR analysis were consistent with the expression profiles determined by microarray analysis.

Statistical Analysis of Gene Expression Data and Identification of Genes Representing Modulated Biological Processes and Molecular Functions. The results of the PCA plot show that major sources of data variability were due to the exposure (air or phosgene) and the time of exposure. This information was used to design an ANOVA using exposure, time, and sample. The genes were ranked by p value based on this three-way mixed model ANOVA. Supporting Information Figure 4 and Supporting Information Table 2 report the most significantly changed genes over time and dose at $p < 0.001$. To determine genes that represent molecular functions and biological processes that were most affected by phosgene exposure, the genes most significantly changed in expression level over time and dose ($p < 0.001$) were mapped to the Gene Ontology (GO) (17). The GO project is a collaborative effort to address the need for consistent descriptions of gene products in different databases and utilizes a controlled GO vocabulary in a curated database. GO provides three structured networks of defined terms to describe gene product attributes: biological process, molecular function, and cellular compartment. We used the web-based search engine Onto-Express to map our genes to the GO database (15). Onto-Express translates lists of differentially regulated genes identified in high throughput gene expression experiments into statistically significant functional profiles based on the GO. Supporting Information Table 3 summarizes genes that represent the molecular functions most affected by phosgene exposure ($p < 0.01$), and Supporting Information Table 4 summarizes the genes that represent the biological processes most affected by phosgene exposure ($p < 0.01$).

Effects of Phosgene Exposure on Antioxidant Enzymes. The effect of phosgene or air exposure on the temporal profile of gene expression for the elements of the GSH redox cycle and SOD is shown in Figure 1. GSH-S-transferase (GST) α -2 follows an expected pattern in that overall expression levels are enhanced within the first 24 h after exposure, with the highest expression measured within about 4 h of exposure, but approximate control values in 2–3 days (Figure 1A). Overall, there was a significant gas exposure by time interaction at a level of $p < 7.2 \times 10^{-22}$ (three-way ANOVA).

GPx-2, which is important in the conversion of reduced GSH into the oxidized form GSSG, shows a significant temporal increase in RNA expression between 4 and 12 h after exposure (Figure 1B). This enhanced expression in phosgene-exposed samples is observed 12–48 h after exposure. There was a significant gas exposure by time interaction at a level of $p < 1.6 \times 10^{-22}$ (three-way ANOVA).

The temporal profile of glutamate cysteine ligase (GCL) subunit gene expression in mice is shown in Figure 1C. There was a significant gas exposure by time interaction at a level of $p < 2.8 \times 10^{-22}$ (three-way ANOVA). The expression level of GCL begins to significantly increase after 0.5 h and is higher than levels in the 8 h time point-matched air-exposed mice. From 24 to 72 h, GCL gene expression trends toward the levels observed in controls but remains elevated.

GR, which catalyzes the reduction of GSSG back to the reduced form of GSH, also shows a significant gas

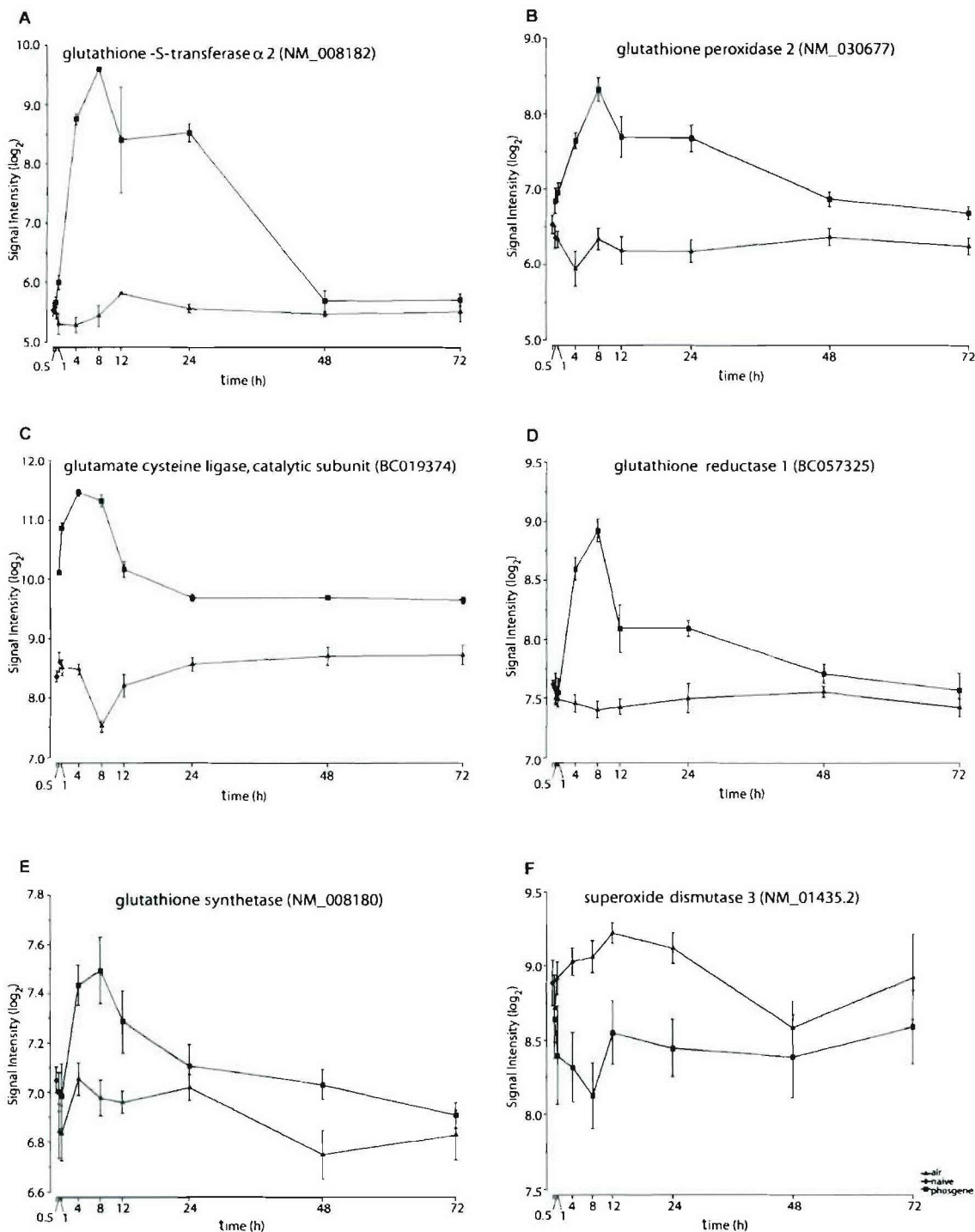


Figure 1. Genes related to antioxidant response after pulmonary exposure to phosgene. Genes known to be involved in the antioxidant response were analyzed using oligonucleotide microarrays. The \log_2 signal intensity represents gene expression level. Sample sizes were three mice per time point for air or phosgene, and replicate chips were probed. Data are expressed as means \pm SEM. (A) GST α -2 gene expression in mice. There was a significant exposure treatment by time interaction at a level of $p < 7.2 \times 10^{-22}$ (three-way ANOVA). (B) GPx-2 gene expression in mice. There was a significant exposure treatment by time interaction at a level of $p < 1.6 \times 10^{-22}$ (three-way ANOVA). (C) GCL subunit gene expression in mice. This gene is also referred to as γ -glutamyl cysteine synthetase, the rate-limiting enzyme required for GSH formation. There was a significant exposure treatment by time interaction at a level of $p < 2.8 \times 10^{-22}$ (three-way ANOVA). (D) GR gene expression in mice. There was a significant exposure treatment by time interaction at a level of $p < 2.9 \times 10^{-16}$ (three-way ANOVA). (E) GS gene expression in mice. There was a significant exposure treatment by time interaction at a level of $p < 1.9 \times 10^{-6}$ (three-way ANOVA). (F) Extracellular SOD3 gene expression in mice. There was a significant decrease in the exposure challenge by time interaction at a level of $p < 2.2 \times 10^{-5}$ (three-way ANOVA).

exposure by time interaction at a level of $p < 2.9 \times 10^{-16}$ (three-way ANOVA; Figure 1D). While the effect was not as pronounced as that observed with GPx, there was nonetheless a significant change in GR gene expression levels in the 4–12 h postexposure range as compared with air-exposed controls.

GS gene expression levels were greater than time-matched air-exposed controls across all time points with the most dramatic increases observed in the 4–24 h time frame (Figure 1E). Overall, there was a significant gas exposure by time interaction at a level of $p < 1.9 \times 10^{-6}$ (three-way ANOVA).

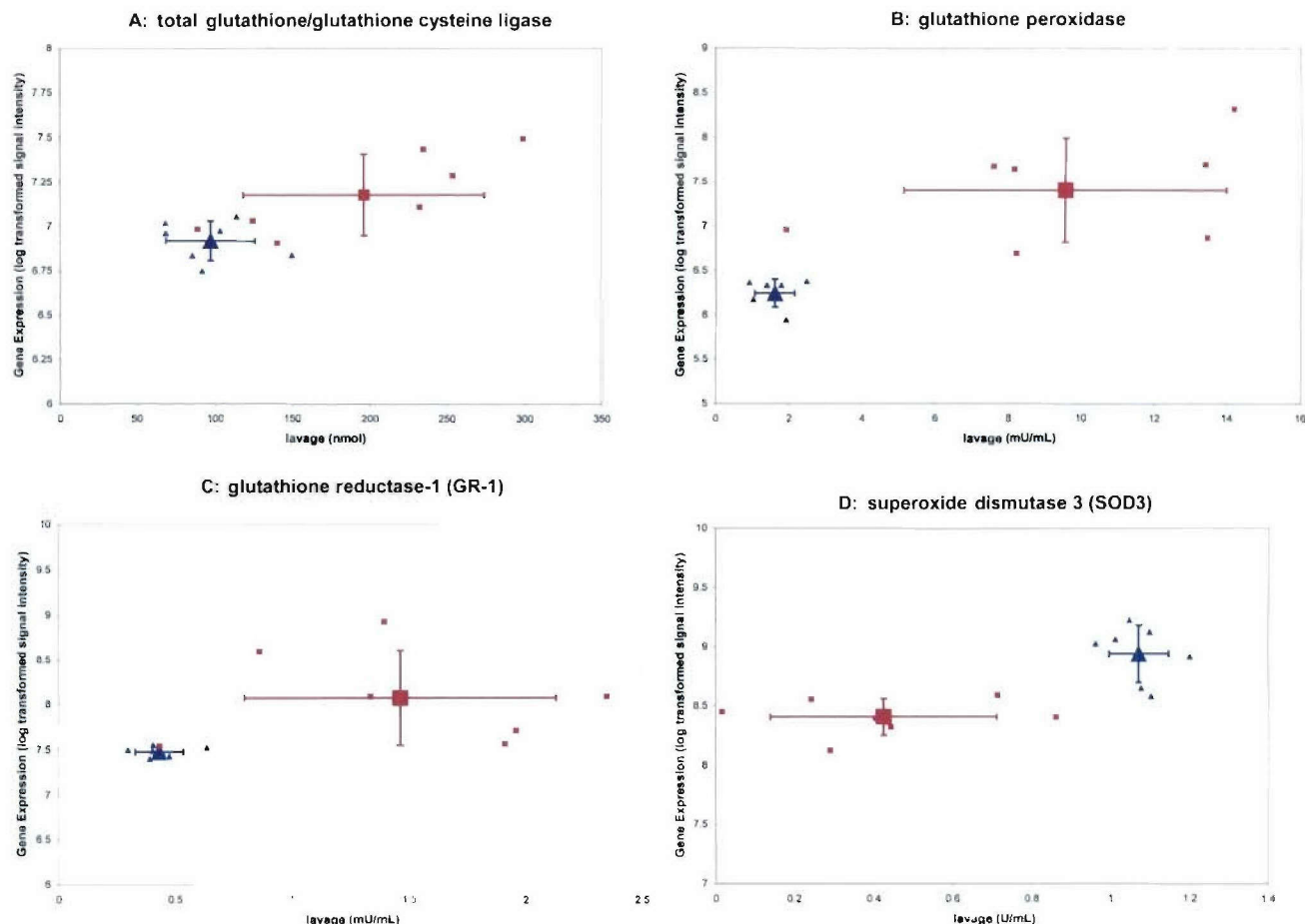


Figure 2. Correlation between gene expression and biochemical analyses. The correlation between microarray gene expression data from phosgene-exposed mouse lung tissue in this study and biochemical data from phosgene-exposed mouse lung BALF generated in our earlier study (21) is shown. (A) Average of the gene expression data (ordinate, \log_2 signal intensity) plotted against the average of the BALF data (abscissa) for total glutathione/glutathione cysteine ligase for air (\blacktriangle) and phosgene-exposure (\blacksquare). The smaller \blacktriangle and \blacksquare represent the individual values from individual experiments for each gas exposure treatment. (B) GPx, (C) GR1, and (D) SOD3. Sample sizes for the microarray analysis were $n = 6$ (three samples run in duplicate) and $n = 7$ (each sample run in duplicate) for the biochemical BALF studies.

The effect of phosgene or air exposure on the temporal profile of extracellular SOD3 gene expression in mice is shown in Figure 1F. In contrast to all other antioxidant response enzymes in this injury model, there was a significant decrease in the expression level of SOD3 after phosgene exposure at a level of $p < 2.2 \times 10^{-5}$ (three-way ANOVA) in a gas exposure by time interaction. Decreased expression levels were persistent through 48 h.

Cross-Validation of Data from Lung Tissue Microarray vs BALF Biochemical Analyses. Cross-validation of independent techniques using lung tissue RNA microarray analyses in this study vs bronchoalveolar lavage (BALF) biochemical data from our previous work (21) is shown in Figure 2. The data are plotted as statistical means from both analytical methods over the course of 72 h. The catalytic subunit GCL (also known as γ -glutamylcysteine synthetase) as compared to GSH levels is shown in Figure 3A. We did not measure GCL in the initial BALF studies, but because it is the rate-limiting enzyme in GSH synthesis (23), it should serve as an appropriate indicator of GSH formation. It is clear that phosgene exposure caused an increase in the expression levels of GCL that matches the increased levels determined for BALF GSH from the initial study (21). In fact, both GPx (Figure 2B) and GR1 (Figure 2C) show considerable agreement between enzyme activity in

BALF and gene expression levels determined in lung tissue. SOD3 (Figure 2D) shows the opposite effect in that exposure to phosgene reduces both enzymatic activity as measured in BALF and gene expression levels in lung tissue. GSH transferase was not included here because it was not measured in the original BALF study.

Discussion

This study utilized oligonucleotide microarrays to determine global changes in gene expression in the murine lung following phosgene exposure. These microarray data confirm biochemical changes that have been studied previously (GSH biosynthesis) but also reveal other biological processes involved in phosgene toxicity, including angiogenesis, cell death, cholesterol biosynthesis, cell adhesion, and cell cycle regulation. Future studies will examine the role of these processes in phosgene toxicity.

We focused further on two important biological responses resulting from an inhalation exposure to phosgene. First, we have clearly demonstrated that gene expression levels for antioxidant enzymes centered on GSH activity are significantly altered in lung tissue over time. Second, we have quantitatively linked changes in gene expression determined in exposed lung tissue with results from another biological medium, BALF. The

agreement between these two analytical methods supports the original hypothesis that one of the most significant and early effects of phosgene exposure is alteration of enzymatic pathways that aid in detoxification of reactive free radical species. This may be the case particularly with the reduction in SOD expression and activity, which may indicate that this specific detoxification system is overwhelmed by superoxide anion formation. The fact that GSH is lower in the tissue and higher in the BALF has been determined previously in rodents and humans (5, 24).

The role of the endogenous critical intra- and extracellular antioxidant GSH and of the redox cycle that regulates its formation has been investigated in lung tissue following exposure to phosgene (10). GSH and the enzymes that help to regulate its availability in the biologically advantageous reduced form have been investigated under numerous lung cell or tissue stress conditions. Exposure to hydrogen peroxide or asbestos/silica has been shown to produce changes in antioxidant enzyme expression levels that signal an imbalance in the protective ratio of antioxidants to oxidative processes (18, 19). In transgenic studies, Ho et al. have shown that mice deficient in GPx are more susceptible to acute paraquat toxicity (20). Historically, we have determined that the most severe phosgene-induced acute lung injury in this model ranges from 4 to 12 h after exposure (8–12). These determinations were made at the physiological, toxicological, histopathological, and/or biochemical levels. Furthermore, within this time frame, the greatest unfavorable changes in the GSH redox cycle and related antioxidant enzyme activities are observed. We have recently demonstrated in mouse lung lavage fluid analysis that exposure to phosgene caused enhanced GPx, GSH, and GR but decreased SOD over time as measured by ELISA and kinetic assays (21).

The homeostatic balance between antioxidant and oxidant levels in vivo is critical in the pathogenesis of oxidative lung injury. The principal cellular thiol regulator of this equilibrium is GSH. GSH has been well-studied and can react both enzymatically and chemically with many electrophilic compounds. In the present study, we have investigated the role of the GSH redox cycle constituents at the gene expression level. In the case of GPx, it has been shown that enhanced production of GPx may be linked to increased gene expression in response to oxidative stress (22). As a result, we have clearly shown that the GSH redox cycle and GSH transferase detoxification processes are highly active over time in this oxidative injury model.

In conclusion, we determined that exposure to phosgene causes oxidative injury in lung tissue over time as determined by microarray analysis and Q-PCR. Of the genes examined, it appears that the gene expression level of the rate-limiting enzyme in GSH synthesis, GCL, is significantly altered, suggesting that the lung is attempting to favorably regulate the antioxidant/oxidant ratio by increasing GSH synthesis, especially at 4–24 h postexposure. Both GR and GPx, which are important in the GSH redox cycle, are also significantly enhanced between 4 and 12 h after exposure. These data suggest that there may be a surplus of formed reactive oxidative species that is causing reduced GSH to be consumed, resulting in the subsequent turnover to GSSG. Furthermore, these data also suggest that GR expression is enhanced in an attempt to reestablish protective levels

of reduced GSH. In addition, SOD gene regulation is significantly decreased over time. This is possibly in response to the enhanced production of superoxide anion free radicals. GSH transferase levels are significantly higher in phosgene-exposed animals than in air-exposed animals from 4 to 24 h, indicating that GSH-conjugated detoxification pathways are active. Data described herein support earlier in vivo BALF studies that demonstrate that oxidative injury caused by phosgene may be regulated at the gene expression level of the GSH redox cycle. This regulation may be mechanistically determined in the tissue at the molecular level by the presence of free radicals and/or a decrease in the signal transduction coupled to cellular antioxidant to oxidant proportion.

Acknowledgment. We thank Albert Sylvester for his excellent research assistance, Richard Sweeney for help in information management, Robyn Lee for statistical support, and Gary Minsavage and Dana Anderson for critical reading of the manuscript. The opinions or assertions contained herein are the private views of the authors and are not to be construed as official or as reflecting the views of the Army or the Department of Defense. In conducting the research described in this report, the investigators adhered to the Guide for the Care and Use of Laboratory Animals of the Institute of Laboratory Animal Resources, National Research Council, in accordance with stipulations mandated for an AAALAC accredited facility.

Supporting Information Available: Tables of primers and probes used for Q-PCR analysis of selected genes, genes most significantly (Bonferroni-corrected, $p < 0.0001$) modulated by exposure to phosgene, genes that represent the molecular functions most affected by phosgene exposure ($p < 0.01$), and genes that represent the biological processes most affected by phosgene exposure ($p < 0.01$). Figures of gene expression data from phosgene-exposed mouse lungs analyzed by PCA; air-exposed and phosgene-exposed samples analyzed separately by PCA; relative expression levels of GPx 2, GR-1, GS, and SOD3 based on Q-PCR analysis; and most significantly changed genes over time and dose at $p < 0.001$. This material is available free of charge via the Internet at <http://pubs.acs.org>.

References

- (1) National Institute of Occupational Safety and Health (1993) *Criteria for a Recommended Standard: Occupational Exposure to Phosgene*, Publication 76137, NIOSH, Washington, DC.
- (2) Brown, J. E., and Birky, M. M. (1980) Phosgene in the thermal decomposition products of poly(vinyl chloride): Generation, detection, and measurement. *J. Anal. Toxicol.* **4**, 166–174.
- (3) Krajewski, J. A. (1997) Chemical accidents and catastrophes as a source of the greatest hazards to the environment and human health. *Med. Pr.* **48**, 93–103.
- (4) Borak, J., and Diller, W. F. (2000) Phosgene: Mechanisms of injury and treatment strategies. *J. Occup. Environ. Med.* **43**, 110–119.
- (5) Sciuto, A. M. (1998) Assessment of early acute lung injury in rodents exposed to phosgene. *Arch. Toxicol.* **72**, 283–288.
- (6) Sciuto, A. M., Strickland, P. T., and Gurtner, G. H. (1998) Postexposure treatment with isoproterenol attenuates pulmonary edema in phosgene-exposed rabbits. *J. Appl. Toxicol.* **18**, 321–329.
- (7) Reid, F. M., Sciuto, A. M., Truxall, J. A., Neimuth, N., Vesely, K. R., and Stotts, R. R. (2000) A 72-hour anesthetized, ventilated swine model to assess efficacy of treatments for respiratory casualties. *BioSci. Proc. III*, 1387–1397; USAMRICD, APG, MD.
- (8) Sciuto, A. M., Moran, T. S., Narula, A., and Forster, J. S. (2001) Disruption of gas exchange in mice following exposure to the chemical threat agent phosgene. *Military Med.* **160**, 809–814.
- (9) Duniho, S. M., Martin, J., Forster, J. S., Cascio, M. B., Moran, T. S., Carpin, L. B., and Sciuto, A. M. (2002) Acute pulmonary changes in mice exposed to phosgene. *Toxicol. Pathol.* **30** (3), 339–349.

- (10) Sciuto, A. M., Lee, R. B., Forster, J. S., Cascio, M. B., and Moran, T. S. (2002) Temporal changes in respiratory dynamics in mice exposed to phosgene. *Inhalation Toxicol.* 14, 487–501.
- (11) Sciuto, A. M., Carpin, L., Moran, T., and Forster, J. (2003) Chronological changes in electrolyte levels in arterial blood and bronchoalveolar lavage fluid in mice after exposure to an edemagenic gas. *Inhalation Toxicol.* 15, 663–674.
- (12) Sciuto, A. M., Clapp, D., Hess, Z., and Moran, T. (2003) The temporal profile of cytokines in the bronchoalveolar lavage fluid in mice exposed to the industrial gas phosgene. *Inhalation Toxicol.* 15, 687–700.
- (13) Sciuto, A. M., Strickland, P. T., Kennedy, T. P., and Gurtner, G. H. (1995) Protective effects of *N*-acetylcysteine treatment after phosgene exposure in rabbits. *Am. J. Respir. Crit. Care Med.* 151, 768–772.
- (14) Sciuto, A. M. (1997) Ibuprofen treatment enhances the survival of mice following exposure to phosgene. *Inhalation Toxicol.* 9, 389–403.
- (15) Khatri, P., Draghici, S., Ostermeier, G. C., and Krawetz, S. A. (2002) Profiling gene expression using Onto-Express. *Genomics* 79, 266–270.
- (16) Applied Biosystems (2001) *Applied Biosystems: User Bulletin #2*, ABI PRISM 7700 Sequence Detection System, Foster City, CA.
- (17) The Gene Ontology Consortium (2000) Gene ontology: Tool for the unification of biology. *Nat. Genet.* 25, 25–29.
- (18) Pietarinen-Runtti, P., Lakari, E., Raivo, K. O., and Kinnula, V. L. (2000) Expression of antioxidant enzymes in human inflammatory cells. *Am. J. Physiol. Cell Physiol.* 278, C118–C125.
- (19) Janssen, Y. M. W., Marsh, J. P., Absher, M. P., Hemenway, D., Vacek, P. M., Leslie, K. O., Borm, P. J. A., and Mossman, B. T. (1992) Expression of antioxidant enzymes in rat lungs after inhalation of asbestos or silica. *J. Biol. Chem.* 267 (15), 10625–10630.
- (20) Ho, Y.-S., Magnenat, J.-L., Gargano, M., and Cao, J. (2000) The nature of antioxidant defense mechanisms: A lesson from transgenic studies. *Environ. Health Perspect.* 106 (Suppl. 5), 1219–1228.
- (21) Sciuto, A. M., Cascio, M. B., Moran, T., and Forster, J. (2003) The fate of antioxidant enzymes in bronchoalveolar lavage fluid over 7 days in mice with acute lung injury. *Inhalation Toxicol.* 15, 675–685.
- (22) McCusker, K., and Hoidal, J. (1990). Selective increase of antioxidant enzyme activity in the alveolar macrophages from cigarette smokers and smoke exposed hamsters. *Am. Rev. Respir. Dis.* 141, 678.
- (23) Tian, L., Shi, M. M., and Forman, H. J. (1997) Increased transcription of the regulatory subunit of γ -glutamylcysteine synthetase in rat lung epithelial L2 cells exposed to oxidative stress or glutathione depletion. *Arch. Biochem. Biophys.* 342 (1), 126–133.
- (24) Cantin, A. M., North, S. L., Hubbard, R. C., and Crystal, R. G. (1987) Normal alveolar epithelial lining fluid contains high levels of glutathione. *J. Appl. Physiol.* 63, 152–157.

TX050126F